An Analytical 2D Current Model of Double−Gate Schottky−Barrier MOSFETs

Yu Ning Zhao[1,2,*], Gang Du[1], Jin Feng Kang[1], Xiao Yan Liu[1,†] and Ruqi Han[1]
Institute of Microelectronics[1], Shenzhen Graduate School[2]
Peking University
Beijing, China[1], Guangdong, China[2]
*zhaoyuning@ime.pku.edu.cn, †xyliu@ime.pku.edu.cn

Abstract—**In this paper, an analytical 2D current model of Double−Gate Schottky−Barrier MOSFETs (DG SB MOSFETs) is developed, which takes the advantage of the 2D potential distribution. Simulation results have shown that current density undergo notable changes along the channel depth directions, indicating that I_{ds} and V_{th} calculated by 2D current model achieve a better accuracy than Surf model**

Keywords−Schottky−Barrier; 2D potential distribution; Tunneling current

I. INTRODUCTION

Schottky Barrier source/drain (S/D) field−effect transistors (SB MOSFETs) are promising substitutes for conventional MOSFETs for sub−22−nm CMOS technology since silicide S/D can provide abrupt junctions with low series resistance [1−3]. Schottky−Barrier MOS technology has advanced significantly in the past ten years [4]. Many experiments and modeling works have been addressed for better understanding and fabrication of the SB MOSFETs. However, few works have addressed the analytical current model for SB MOSFETs. Here we present an analytical 2D current model of Double−Gate (DG) SB MOSFETs. Our current model takes advantage of the 2D potential distribution, especially the 2D distribution of the Schottky barrier shape, instead of surface potential. The 2D potential distribution and I_{ds} are verified by the simulated results of DESSIS [5], and the threshold voltage is extracted from I_{ds}. Different threshold voltages extracted from different I_{ds} models are compared.

II. MODELING

First we consider the tunneling current model for DG SB MOSFET, since it is the dominant current in SB MOSFETs [6]. Two main methods exist for the calculation of tunneling current through the barrier: the WKB method and the Airy function method. Here we take WKB since it fits the situation of high barrier and is simpler to implement [6]. In the WKB method, the tunneling transmission probability $T(p_x)$ is so sensitive to the barrier shape that a modeling of potential distribution in DG SB MOSFETs with high accuracy is required, especially near the Schottky barrier region. Fig.1(a) gives a schematic view of the DG SB MOSFET structure, where the channel length L_x is 50nm, Silicon thin film thickness T_{si}=10nm, Gate dielectrics thickness EOT=1nm and Donor doping concentration N_d=10^{17}cm^{-3}. Fig.1(b) where the electric potential distributions and tunneling current densities along the channel depth directions are demonstrated schematically, reveals that the variances of Schottky barrier shapes in different y-slices result in remarkable variances of tunneling current density.

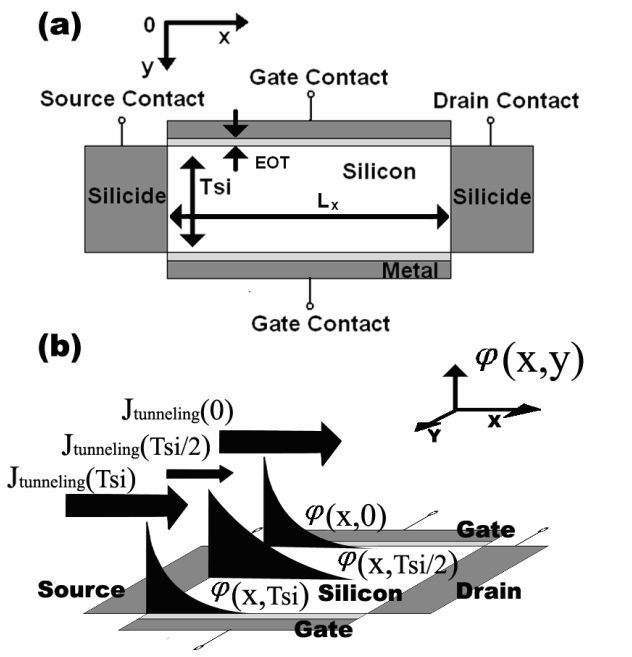

Figure 1. (a). Schematics of DG SB MOSFET. (b). Schematics of tunneling current density and electric potential near the source side.

The 2D potential expression is solved from the Poisson Equation [7] under the following boundary conditions:

$$\varphi(x,0) = \varphi_1(x) \tag{1a}$$

$$\partial\varphi/\partial y \,|_{y=a} = 0 \tag{1b}$$

$$\varphi(0,y) = \varphi_1(0) \tag{1c}$$

$$\varphi(x,\lambda) = \varphi_1(\lambda) \tag{1d}$$

978-1-4244-1753-7/08/$25.00 ©2008 IEEE

where $a = T_{si}/2$, $\lambda=L_x/2$, $\varphi_{sL}=V_{gs}+q\,N_d\,t_{s\,i}\,EOT/(2\varepsilon_{SiO2})$, $l=(\varepsilon_{Si}\,T_{si}\,EOT/(2\,\eta\,\varepsilon_{SiO2}))^{0.5}$, $\varphi_l(x)=\varphi_{sL}+(V_{bi}+V_{gs}-\varphi_{sL})exp(-x/l)$, $\eta=E(x,0)/E_{average}(x)$ and E is electric field in the x direction. The solution of this equation is eq.2.

$$\varphi(x,y)=\varphi_l(0)+\frac{\varphi_l(\lambda)-\varphi_l(0)}{\lambda}x+\frac{qN_d}{2\varepsilon_{si}}(\lambda-x)x+$$
$$\sum_{n=0}^{\infty}\frac{-4N_d\lambda^2}{\varepsilon_{si}\left[(2n+1)\pi\right]^3}\sin\left(\frac{(2n+1)\pi x}{\lambda}\right)\frac{\cosh\left((2n+1)\pi(a-y)/\lambda\right)}{\cosh\left((2n+1)\pi a/\lambda\right)}+$$
$$\sum_{n=1}^{\infty}\left[\frac{2\beta}{n\pi}(1-\cos n\pi)-\frac{2n\pi\beta}{(\lambda/l)^2+(n\pi)^2}\left(1-\exp(-\frac{\lambda}{l})\cos n\pi\right)+\right.$$
$$\left.\left(2\gamma\lambda\cos n\pi/n\pi\right)\right]\cdot$$
$$\sin\left(\frac{n\pi x}{\lambda}\right)\cdot\frac{\cosh\left(n\pi(a-y)/\lambda\right)}{\cosh\left(n\pi a/\lambda\right)} \quad (2)$$

where $\beta=\varphi_{sL}-V_{bi}$ *and* $\gamma=(\varphi_{sL}-V_{bi}+(V_{bi}-\varphi_{sL})exp(-\lambda/l))/\lambda$. Considering that a single fitting parameter η could not depict the variance along the channel direction, we change η to $\eta(x)$ to get more accurate potential distribution. Then the tunneling probability is written as $T(\varepsilon_x,y)=\exp(-2\int(2m_{WKB}(\kappa-q(\varphi(x,y)-\varphi(0,y))-\varepsilon_x)/\hbar^2)^{0.5}dx)$. The expression of electron density of states is also essential to calculate the tunneling current. As the states in metal are continuous and the states in semiconductor are quasi−continuous, the electron density of states in metal and semiconductor for calculating tunneling current are determined by the semiconductor side $g(\varepsilon,p_x)=2\pi m/h^3$ [8]. Then, the tunneling current J_t can be written as eq.3 [8]

$$J_t=(2p_x/m_e)\cdot T(p_x)\cdot[g(\varepsilon,p_x)f(\varepsilon-\varepsilon_f^m)(1-f(\varepsilon-\varepsilon_f^s))-g(\varepsilon,p_x)\cdot f(\varepsilon-\varepsilon_f^s)$$
$$(1-f(\varepsilon-\varepsilon_f^m))] \quad (3)$$

where m_e is the effective mass of electron, $T(p_x)$ is the transmission probability, ε is the total energy of electron, p_x is the momentum along channel direction, $f(\varepsilon)$ is the Fermi−Dirac functions, ε_f^m is the Fermi level in metal and ε_f^s is the Fermi level in semiconductor. The total tunneling current is also the sum of the current emission over the barrier (the thermal emission current J_{th}) and current emission through the barrier J_{tun} [4]. The J_{th} can be calculated by classical thermal−emission theory as $J_{th}=A^*T^2exp(-\Phi_{barrier}/KT)\{exp(qV/KT)-1\}$ [4] and the J_{tun} is calculated by eq. 3 under the situation of $E_C<\varepsilon_x<\Phi_{barrier}$. Since the drain current in threshold region of DG SB MOSFETs with positive barrier is determined simply by the electron tunneling current at the Source Contact, the J_{ds} is calculated by summing up the J_{th} and the J_{tun} at the Source side. Fig.2 shows the main flow chart of our current model, and the eq. 4 is the current equation of DG SB MOSFETs in threshold region.

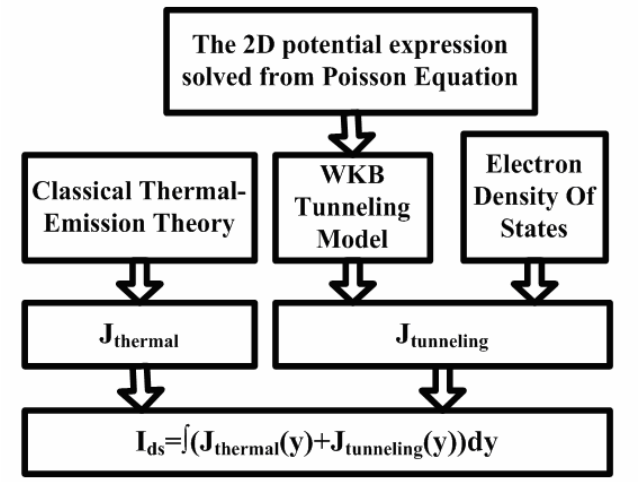

Figure 2. Main flow chart of our 2D current model.

$$J_{ds}(y)=-A^*T^2exp(-\Phi_{barrier}/KT)\{exp((\varepsilon_f^m-\varepsilon_f^s)/KT)-1\}-$$
$$(KT/2\pi^2\hbar^3))\int mT(\varepsilon_x,y)ln((1+exp((\varepsilon_f^m-\varepsilon_x)/KT))/$$
$$(1+\exp((\varepsilon_f^s-\varepsilon_x)/KT)) \quad (4)$$

III. Results and Discussion

In order to verify the tunneling current model, the $J-V$ characteristics of the Schottky Diode (SD) are calculated by our model and the results are compared with the simulated results of DESSIS as well as the experimental results [9].

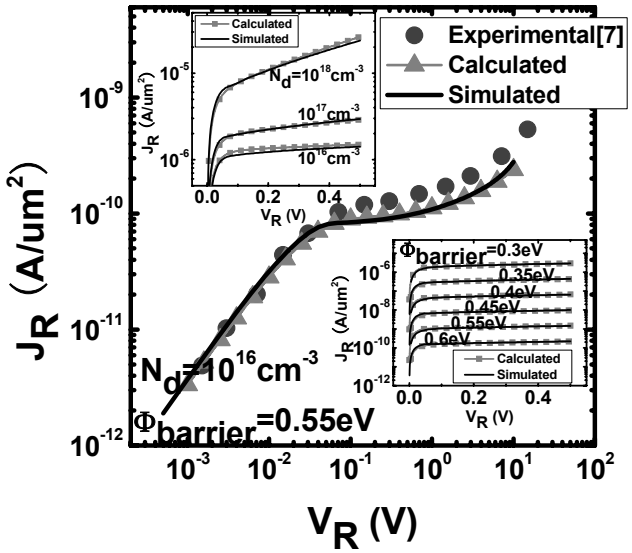

Figure 3. Reverse $J-V$ characteristics of Schottky Diode. Comparison between the results of experiment, DESSIS and our model

Fig.3 shows the comparison results. The insets of Fig.3 show $J-V$ curves with different N_d and $\Phi_{barrier}$ respectively. It can be seen that our model is accurate in most region of SD

$J-V$ curve with various parameters as barrier height and dopant concentration.

Fig.4 shows the potential distribution in the silicon thin film with different gate bias and different depth varied from 0 to 5nm (step=1nm) from the Si/SiO_2 interface. A good agreement is achieved between the results of the potential model and DESSIS results.

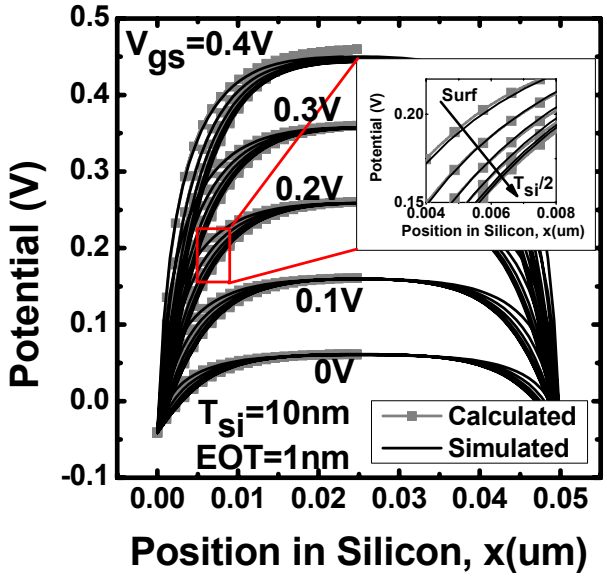

Figure 4. Potential in silicon thin film of DG SB MOSFETs with different V_{gs} and depth varied from 0 to 5nm (step=1nm) from the surface.

Fig.5 shows the current density in different slices along y direction in the silicon film of DG SB MOSFETs. It is interested to note that the changes of depth do induce large variances of the tunneling current density, and the value of $J_{ds}(y)/J_{ds,average}$ is not fixed but varies with V_{gs}, so the current model should be established including 2D distribution.

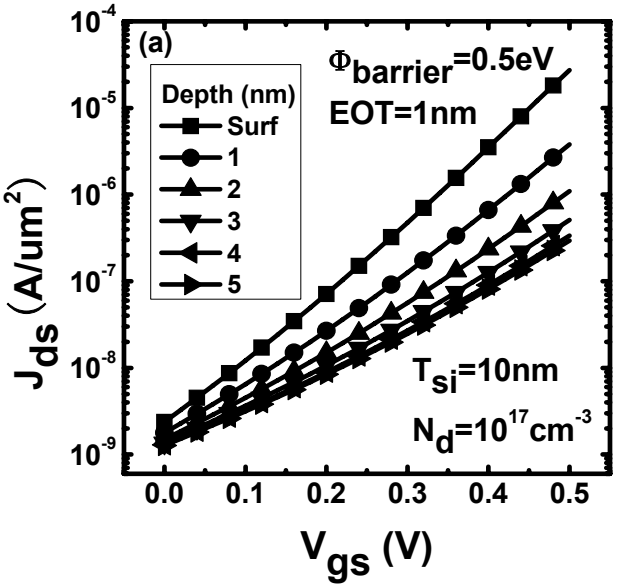

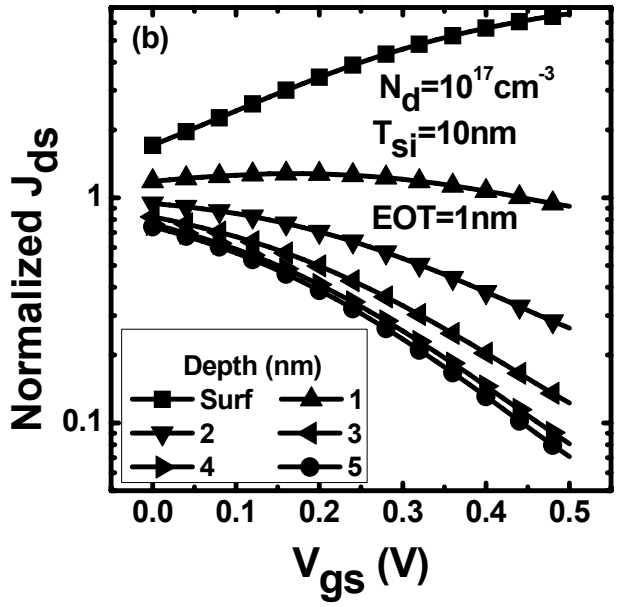

Figure 5. (a). Current density in different slices along y direction in the silicon film of DG SB MOSFETs. (b). The current density in different slices along y direction in the silicon film normalized by the average current density.

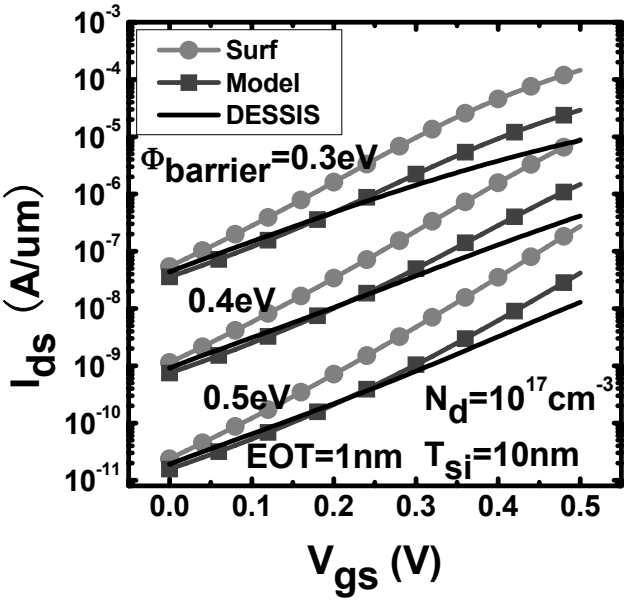

Figure 6. I_{ds}–V_{gs} characteristics of the DG SB MOSFETs with different $\Phi_{barrier}$.

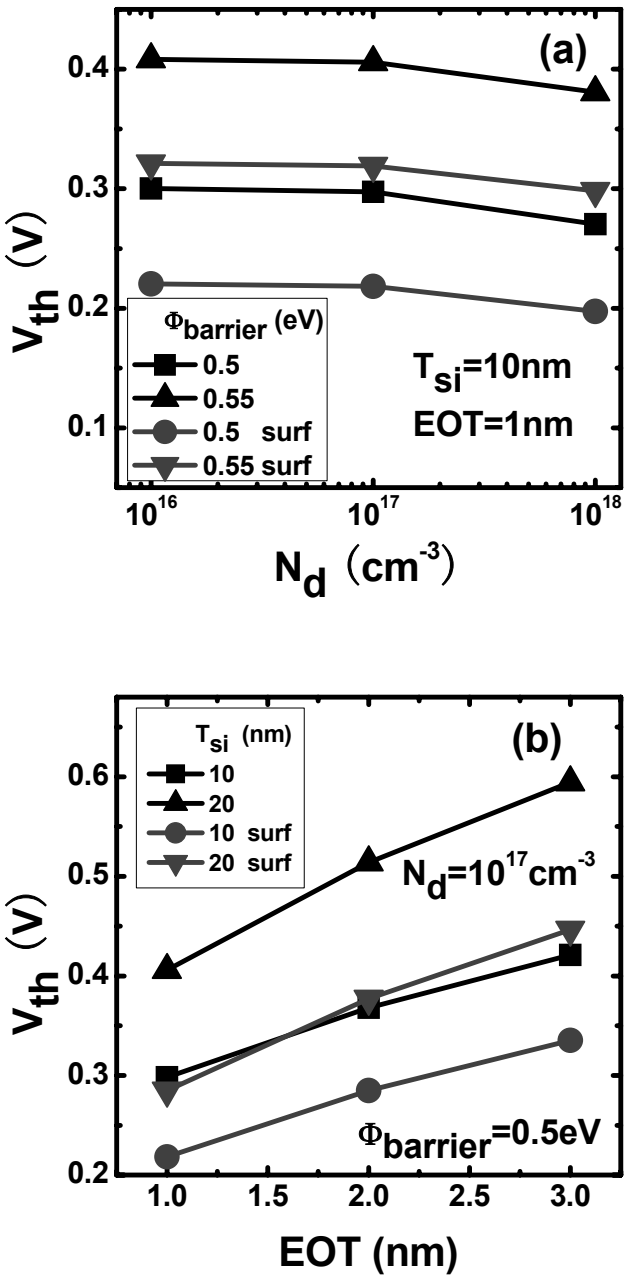

Figure 7. (a). Variances of V_{th} @ I_{ds}=10^{-9}A/um with different T_{si} and EOT. (b). Variances of V_{th} @ I_{ds}=10^{-9}A/um with different N_d and $\Phi_{barrier}$.

Fig.6 shows the I_{ds}−V_{gs} characteristics of the DG SB MOSFETs with different $\Phi_{barrier}$, and the results of surface current and the simulated results of DESSIS are compared. It is obvious that our model matches the simulated results better than the model (Surf) that only takes surface current into account.

Figs 7(a), (b) plot the variances of V_{th} with different N_d, T_{si}, EOT and $\Phi_{barrier}$ calculated by our current model and by Surf model. The linear extrapolation of the I_{ds}−V_{gs} for determining V_{th} is not suitable for DB SB MOSFETs, as the I_{ds} exponentially increases with the V_{gs}. We use the constant current method to determine the V_{th}. From these two figures and compared with the results in reference 10, we find that the calculated results of V_{th} by our model are proper and the variances of V_{th} are reasonable.

IV. Conclusion

An analytical 2D current model of DG SB MOSFETs is developed. It takes advantage of the 2D potential distribution. Results indicate that the current density changes significantly with the variances of the depth from the surface, and the Ids and Vth calculated by 2D current model give a better accuracy than Surf model.

Acknowledgment

This work is supported by NKBRP2006CB302705 and 107003.

References

[1] J. Kedzierski, P. Xuan, E.H. Andersonf, J. Bokor, Tsu−Jae King, Chenming Hu, "Complementary silicide source/drain thin−body MOSFETs for the 20 nm gate length regime," IEDM Tech. Dig. 2000, pp. 57−60.

[2] C.−K. Huang, W.E. Zhang, C.H. Yang, "Two−Dimensional Numerical Simulation of Schottky Barrier MOSFET with Channel Length to 10 nm," IEEE T. Electron Dev., vol.45, pp. 842−848, April 1998.

[3] B. Winstead, U. Ravaioli, "Simulation of Schottky Barrier MOSFET's with a Coupled Quantum Injection/Monte Carlo Technique," IEEE T. Electron Dev., vol.47, pp. 1241−1246, June 2000.

[4] J.M. Larson, J.P. Snyder, "Overview and status of metal S/D Schottky−barrier MOSFET technology," IEEE T. Electron Dev., vol. 53, pp. 1048−1058, May 2006.

[5] DESSIS, ISE TCAD Manuals, Integ. Syst. Engr. AG. Zurich, Switzerland.

[6] R.A.Vega, "Comparison study of tunneling models for Schottky field effect transistors and the effect of Schottky barrier lowering," IEEE T. Electron Dev., vol. 53, pp. 1593−1600, July 2006.

[7] Z.−H. Liu, C. Hu, J.−H. Huang, T.−Y. Chan,; M.−C. Jeng, P.K. Ko, Y.C. Cheng, "Threshold voltage model for deep−submicrometer MOSFETs," IEEE T. Electron Dev., vol. 40, pp. 86−95, January 1993.

[8] A.T. Fromhold, Quantum Mechanics For Applied Physics And Engineering. New York, NY: Academic Press, 1981.

[9] J. M. Andrews and M. P. Lepselter, "Reverse current−voltage characteristics of metal−silicide Schottky diodes," Solid−State Electron., vol. 13, pp. 1011−1023, 1970

[10] J. Knoch, M. Zhang, S. Mantl, J. Appenzeller, "On the performance of single−gated ultrathin−body SOI Schottky−barrier MOSFETs," IEEE T. Electron Dev., vol. 53, pp. 1669− 1674, July 200